Cancer Letters 455 (2019) 26–35

Contents lists available at ScienceDirect

Cancer Letters

journal homepage: www.elsevier.com/locate/canlet

FOXO3a knockdown promotes radioresistance in nasopharyngeal carcinoma by inducing epithelial-mesenchymal transition and the Wnt/β-catenin signaling pathway

Min Luo[b], Cheng Wu[a], Ergang Guo[a], Shan Peng[b], Linli Zhang[a], Wei Sun[a], Dongbo Liu[a], Guangyuan Hu[a,*], Guoqing Hu[a,**]

[a] Department of Oncology, Tongji Hospital, Tongji Medical College, Huazhong University of Science and Technology, Hubei, Wuhan, People's Republic of China
[b] Department of Radiation and Medical Oncology, Zhongnan Hospital of Wuhan University, Wuhan, China

ARTICLE INFO

Keywords:
NPC
FOXO3a
Radioresistance
Epithelial-mesenchymal transition
Wnt

ABSTRACT

Mutations in the forkhead box O 3a (FOXO3a) gene are closely related to the progression of several types of cancers. However, few studies explore the relationship between FOXO3a and nasopharyngeal carcinoma (NPC). Our findings demonstrate that silencing FOXO3a promotes tumor radioresistance of NPC in vitro and *in vivo* through inducing EMT and activating Wnt/β-catenin signal pathway. These data establish that FOXO3a can be a novel and reliable NPC marker and a potential therapeutic target against NPC.

1. Introduction

Nasopharyngeal carcinoma (NPC), arising from nasopharyngeal epithelial cells, is an epidemic malignancy with remarkable geographic and ethnic distributions worldwide. Epstein-Barr virus (EBV) exposure, diet, and genetic factors are mainly responsible for the occurrence of NPC in South China [1]. Overall, the prognosis of NPC has dramatically improved over the past three decades owing to better radiotherapy (RT) technology, broader application of chemotherapy, and more accurate disease staging [2]. However, tumor invasion and radioresistance are still major hurdles for a successful treatment [3]. The exact mechanisms underlying tumor invasion and radioresistance of NPC need to be explored further.

The forkhead box O (FOXO) family of proteins has recently been shown to be an important transcriptional regulator of pivotal proteins associated with many diverse cellular functions [4]. FOXO1, FOXO3a, FOXO4, and FOXO6 proteins have already been identified in humans. Compared with other FOXO family members, FOXO3a has been extensively studied because of its unique role in the regulation of cell proliferation, apoptosis, metabolism, stress management, and longevity [5]. FOXO3a gene mutations were found to be closely related to the progression of several types of cancer [6]. However, few studies were carried out to explore the relationship between FOXO3a and NPC. Shou et al. showed that low expression of FOXO3a is significantly correlated with poor prognosis of NPC [7]. The role of FOXO3a in carcinogenesis and NPC prognosis needs to be further elucidated.

An increasing body of evidence suggests that the process of epithelial–mesenchymal transition (EMT) plays an important role in the development of NPC [8,9]. EMT is the process in which epithelial cells lose their epithelial characteristics and acquire a mesenchymal phenotype, which then allows cells to separate from the primary tumor and migrate to other tissues. Moreover, EMT is characterized by loss of the epithelial cell adhesion molecule E-cadherin, which is coupled with increased expression of mesenchyme-associated proteins such as vimentin, N-cadherin, snail, and twist [10]. In addition, FOXO3a has been widely acknowledged to regulate EMT in numerous cancers, except NPC [11,12].

Previous studies have reported that the Wnt/β-catenin signaling

Abbreviations: NPC, nasopharyngeal carcinoma; EBV, Epstein-Barr virus; RT, radiotherapy; FOXO, The Forkhead box O; EMT, epithelial–mesenchymal transition; qRT-PCR, real-time PCR; TUNEL, terminal deoxynucleotidyl transferase-meditated dUTP-fluorescein nick end-labeling; SD, standard deviation; SF2, survival fraction; SER, sensitivity enhancement ratio

* Corresponding author. Department of Oncology, Tongji Hospital, Tongji Medical College, Huazhong University of Science and Technology, 1095 Jiefang Road, Hubei, Wuhan, 430030, China.
** Corresponding author. Department of Oncology, Tongji Hospital, Tongji Medical College, Huazhong University of Science and Technology, 1095 Jiefang Road, Hubei, Wuhan, 430030, China.
E-mail addresses: huguangyuan@tjh.tjmu.edu.cn (G. Hu), huguoqing@tjh.tjmu.edu.cn (G. Hu).

https://doi.org/10.1016/j.canlet.2019.04.019
Received 23 September 2018; Received in revised form 11 April 2019; Accepted 15 April 2019

pathway plays a vital role in tumorigenesis, cisplatin resistance, and prognosis in NPC [8,9,13]. It has also been widely acknowledged that EMT and the Wnt/β-catenin signaling pathway play key roles in cancers becoming radioresistant [14,15]. In addition, FOXO3a has been shown to be strongly correlated with EMT and the Wnt/β-catenin signaling pathway [11,16]. Furthermore, it has been identified to play a vital part in cell cycle arrest, apoptosis, oxidative stress resistance, and autophagy [17–19], all of which are closely related to tumor radioresistance [20–22]. Accordingly, FOXO3a may regulate radioresistance of NPC through these cellular functions. In summary, we hypothesize that FOXO3a affects radioresistance of NPC by inducing EMT, the Wnt/β-catenin signaling pathway and the above mentioned cellular functions associated with them. In this study, we aimed to investigate the underlying mechanisms of tumor radioresistance.

2. Materials and methods

2.1. Cell lines

Human NPC cell lines CNE1, CNE2, HNE1, and CNE1-LMP1 were obtained from the Cancer Research Institute of Central South University (Changsha, China). HNE1 and CNE2 were derived from a poorly differentiated NPC and lost the EBV genome during multiple cell passages [23]. CNE1 is an EBV-negative well-differentiated cell line and CNE1-LMP1 is a stably transfected cell line, established by introducing *LMP1* cDNA into CNE1 cells [24]. The two cell lines, CNE2 and HNE1, used in this study were authenticated using short-tandem repeat profiling, tested for mycoplasma contamination and cultured for less than two months. Cell line authentication was performed according to the suggestions from ATCC cell line authentication. CNE2 and HNE1 cell lines were not contaminated with HeLa. All cell lines were kept in RPMI 1640 media (Promoter Biotech, China) with 10% fetal bovine serum (Gibco, South America) at 37 °C in a humidified 5% CO_2 atmosphere.

2.2. Construction of lentivirus vectors and cell transduction

In order to establish stable transfected cell lines for further experiments, lentivirus vectors were constructed and used for transduction. Lentiviral particles were purchased from GeneChem (GV112, China), and used in the transduction of CNE2 and HNE1 cells following the manufacturer's instructions. Cells were then subcultured in selective medium with 3 mg/mL puromycin (P9620, Sigma, USA) for two weeks to select stable cell lines. Efficiency of transfection was evaluated using western blotting and real-time RT-PCR. The sequences of FOXO3a and mock shRNAs are as follows:

shRNA 1: GCACAACCTGTCACTGCCATAG
shRNA 2: GGAACTGGCAAGAGCTCTTGG
shRNA 3: GCTGTCTCCATGGACAATAGC
Mock shRNA: GCAAGCTGACCCTGAAGTT

The sequences of β-catenin and mock shRNAs are as follows:

β-catenin shRNA: GTGCTATCTGTCTGCTCTA
Mock shRNA: TTCTCCGAACGTGTCACGT

Control cells were co-transduced with FOXO3a mock and β-catenin mock shRNAs.

2.3. X-ray irradiation

An RS2000 X-ray Biological Research Irradiator (3 mm copper filter, 160 kV, 25 mA; Rad Source Technologies, GA, USA) was used to perform X-ray irradiation. The dose rate was 1.151 Gy/min. Single irradiation doses were 2–10Gy.

2.4. Western blotting

Western blotting was used to assess the expression of proteins quantitatively. Total protein was extracted using RIPA buffer (P0013K, Beyotime Biotechnology, China). Nuclear and Cytoplasmic Extraction Reagents (P0027, Beyotime Biotechnology, China) were used to extract nuclear and cytoplasmic proteins following the manufacturer's instructions. Equal amounts of protein, measured using microplate reader (Synergy H1, Biotek, USA) and Beyotime protein assay reagent, were separated using sodium dodecyl sulfate polyacrylamide gel electrophoresis (SDS-PAGE) and transferred to a polyvinylidene fluoride (PVDF) membrane. After blocking, the blots were incubated with the indicated primary antibodies. After washing and incubation with secondary antibodies, the blots were visualized using ECL reagent (NCI4106, Thermo, USA). Anti-FOXO3a (#12829), anti-E-cadherin (#3195), anti-N-cadherin (#13116), anti-vimentin (#5741), anti-snail (#3879), anti-c-Myc (#13987), and anti-lamin B (#12255) were purchased from Cell Signaling Technology (USA), anti-cyclin D1 (ab134175), anti-GSK-3β (ab32391), anti-twist1 (ab175430), and anti-β-catenin (ab32572) were from Abcam, (USA) and anti-GAPDH (AC002) was obtained from Abclonal (USA).

2.5. Real-time PCR

Real-time PCR was applied to detected mRNA expression levels. Total RNA was extracted using Trizol (NO.9766, Takara, Japan) following the manufacturer's instructions. Reverse transcription was performed using the PrimeScript 1st Strand cDNA Synthesis Kit (NO.6110A, Takara, Japan). A Fast Real-Time PCR System (7900HT, Applied Biosystems, USA) was utilized to run real-time PCR (qRT-PCR). Values for individual genes were standardized using GAPDH. A melting curve was obtained for each primer pair to confirm specificity of the amplification product. Primers for PCR were designed by Primer Premier 5.0 software (Premier Biosoft, Palo Alto, CA) as follows:

FOXO3a Forward-CCCAACCAGCTCCTTTAACA;
FOXO3a Reverse-GAGTCCGAAGTGAGCAGGTC;
GAPDH Forward-GGTCGGAGTCAACGGATTTG;
GAPDH Reverse-GGAAGATGGTGATGGGATTTC.

2.6. Scratch test

Scratch test was used to assess the migration abilities of NPC cells. Cells (1×10^5) were placed in 24-well plates for 24 h with 10% fetal bovine serum. Culture medium was then changed to a serum-free medium. A 10-μL pipette tip was used to draw a straight line on the bottom of the 24-well plates. Shifting distances of cells were recorded using inverted microscopy at 200 × magnification at 0 h and 24 h.

2.7. Transwell assay

Transwell assay was employed to test the invasion ability of NPC cells. Boyden chamber assays with 8-μm diameter filters (NO.3422, Corning, USA) were used to detect the invasion abilities of cells. In the upper chamber paved with a layer of matrigel chamber 1×10^5 cells were incubated in approximately 200 μL of serum-free medium. The lower chamber contained 500 μL RPMI 1640 with 10% fetal serum. After incubation for 20–24 h, the lower chamber was fixed in 4% paraformaldehyde for 20 min, stained with crystal violet, and counted under upright microscopy at 200 × magnification (five fields per chamber).

2.8. Immunofluorescence assay

Immunofluorescence assay was employed to test protein localization and expression. Cells were washed three times in phosphate

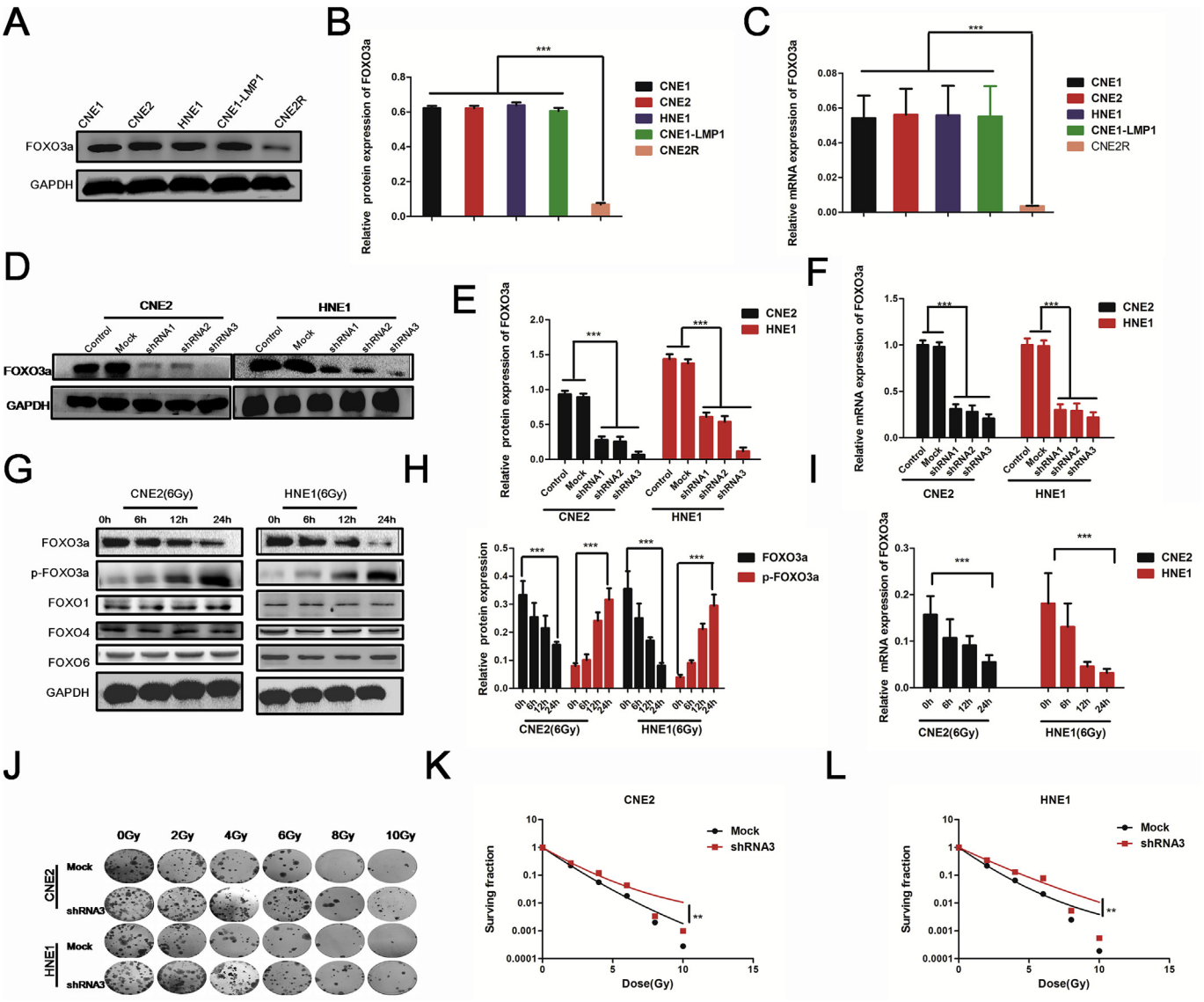

Fig. 1. Knockdown of FOXO3a induces radioresistance in NPC cells. (A–B) FOXO3a protein levels from whole-cell lysates were analyzed using western blotting in different NPC cell lines. (C) Quantification and analysis of FOXO3a mRNA in different NPC cell lines. (D–E) Western blot assays to determine the silencing efficiency of transduced NPC cell lines. (F) Quantification and analysis of FOXO3a mRNA in transduced NPC cell lines. (G–H) The proteins of FOXO family members levels from whole-cell lysates were analyzed using western blotting in different NPC cells after exposure to radiation. (I) Quantification and analysis of FOXO3a mRNA in different NPC cell lines after exposure to radiation. (J) Representative images of colony formation of transfected NPC cells after exposure to radiation. (K–L) Survival curves of clone formation assays of transfected NPC cells. Error bars correspond to means ± standard deviations from three independent experiments. *P < 0.05 vs. control; **P < 0.01 vs. control; ***P < 0.005 vs. control.

buffered solution (PBS), fixed in 4% paraformaldehyde for 10 min, and permeabilized with PBS containing 0.25% Triton for 10 min. After washing three times in PBS, cells were blocked with 1% albumin from bovine serum (BSA) for 30 min. Cells were then incubated overnight at 4 °C with the following antibodies: anti-E-cadherin (#3195, Cell Signaling Technology, USA), anti-vimentin (#5741, Cell Signaling Technology, USA), and anti-β-catenin (ab32572, Abcam, USA). Cells were then stained with second-fluorescence antibody (Alexa 488 and Alexa 594, Life Technologies, USA) at the indicated time points according to the manufacturer's instructions. After three washes in PBS, cells were dyed with 50 Ml 4′,6-diamidino-2-phenylindole (DAPI) at 37 °C for 5 min. Immunofluorescence was examined using an Olympus LX70 fluorescence microscope (Olympus, Japan).

2.9. Colony formation assay

Colony formation assay was used to detect survival fraction in NPC cells after radiation. Cells were seeded at 50, 200,500, 1000, 5000, and 20000 per well in 6-well plates. The plates were then incubated at 37 °C for 24 h for attachment and X-ray irradiated with 0, 2, 4, 6, 8, or 10 Gy. After 10–14 days of incubation for colony formation, the cells were fixed with methanol and then stained with 0.1% crystal violet. The plates were photographed, and the colonies were counted by three different investigators. The experiment was carried out in triplicates for each group. At least 50 cells per clone indicated a valid clone. The survival fraction (%) = number of valid clones/(number of inoculated cells * 0 Gy colony formation rate) * 100%. All related data were inputted in GraphPad Prism 5 software, and survival curves of the clone formation assays were calculated using the single-hit multi-targeted model (y = 1-(1-exp(-k*x))ˆN).

2.10. Apoptosis analysis

Apoptosis analysis was applied to detect the proportion of apoptotic

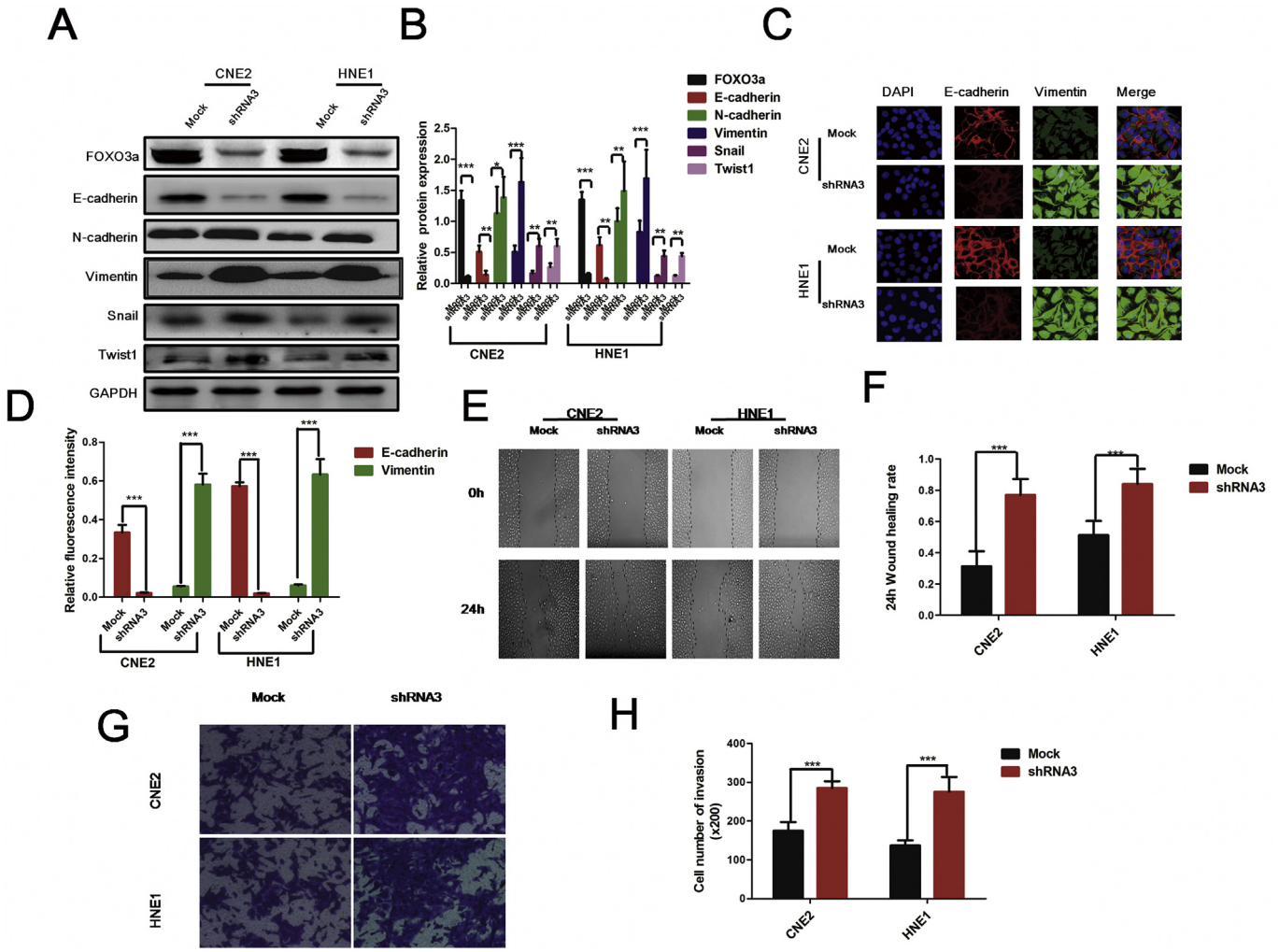

Fig. 2. Silencing of FOXO3a induces EMT in NPC cells. (A–B) EMT-related protein levels from whole-cell lysates were analyzed using western blotting. (C–D) Immunofluorescence assays were used to determine the location of EMT marker proteins. (E) Scratch tests were applied to test the migration ability in transduced NPC cells (magnification: 200 ×). (F) Quantitative assessment of wound-healing rate at the indicated times (0 h and 24 h). (G) Representative images of transwell assays (magnification: 200 ×). (H) Quantitative assessment of the number of cells migrating to the lower chamber. *P < 0.05 vs. control; **P < 0.01 vs. control; ***P < 0.005 vs. control.

NPC cells after radiation. Cells were irradiated with 6 Gy of X-rays and harvested after 48 or 72 h of incubation. FITC Apoptosis Kit (BD556547, BD Biosciences, USA) was used to perform apoptosis analysis following the manufacturer's instructions. Flow cytometry using a FACSort machine (e126037, BD Biosciences, USA) was applied to detect apoptotic cells and CellQuest software was employed to analyze the results.

2.11. Cell cycle analysis

Cell cycle analysis was applied to detect cell cycle distribution in NPC cells after radiation. Cells were exposed to 6 Gy of X-rays and harvested after 24 h or 48 h of incubation. Cell cycle analysis was performed using a Cell Cycle Analysis Kit (BD550825, BD Biosciences, USA) following the manufacturer's instructions. The cells were then analyzed using flow cytometry in a FACS Canto II flow cytometer (e126037, BD Biosciences, USA).

2.12. In vivo xenograft assay

A xenograft mouse model was employed to further validate the results of cell experiments *in vivo*. Four to 6 weeks-old female BALB/c nude mice (Animal Care Center of Hunan SJA Laboratory Animal, Changsha, China) were used. This study was reviewed and approved by the Ethics Committee of Department of Oncology, Tongji Hospital, Tongji Medical College, Huazhong University of Science and Technology. All mice were housed in a specific pathogen-free, temperature and humidity-controlled environment with food and water in their cages. All animal experiments were performed according to the Huazhong University of Science and Technology Animal Care Facility and National Institutes of Health guidelines. In brief, 1.5×10^7 cells in 0.2 mL serum-free RPMI 1640 medium were injected subcutaneously into the right armpit of mice. The animals were randomly divided into 4 groups of 3 animals: untreated CNE2-Mock, untreated CNE2-shRNA3, CNE2-Mock irradiation (CNE2-Mock IR), and CNE2-shRNA3 irradiation (CNE2-shRNA3-IR) groups. Tumors were measured every two days. When the tumors reached 50 mm^3 in dimension, irradiated groups were irradiated with 8 Gy of X-rays. The experiments were then terminated with 4 weeks of tracking.

2.13. Tissue immunohistochemistry

Tissue immunohistochemistry was employed to detect the protein expression of xenograft mouse tissue. Tumor tissues were embedded in paraffin and then cut into 5-μmthick sections. The indicated antibodies and DAB were used to obtain signals from the slides. The In Situ Cell

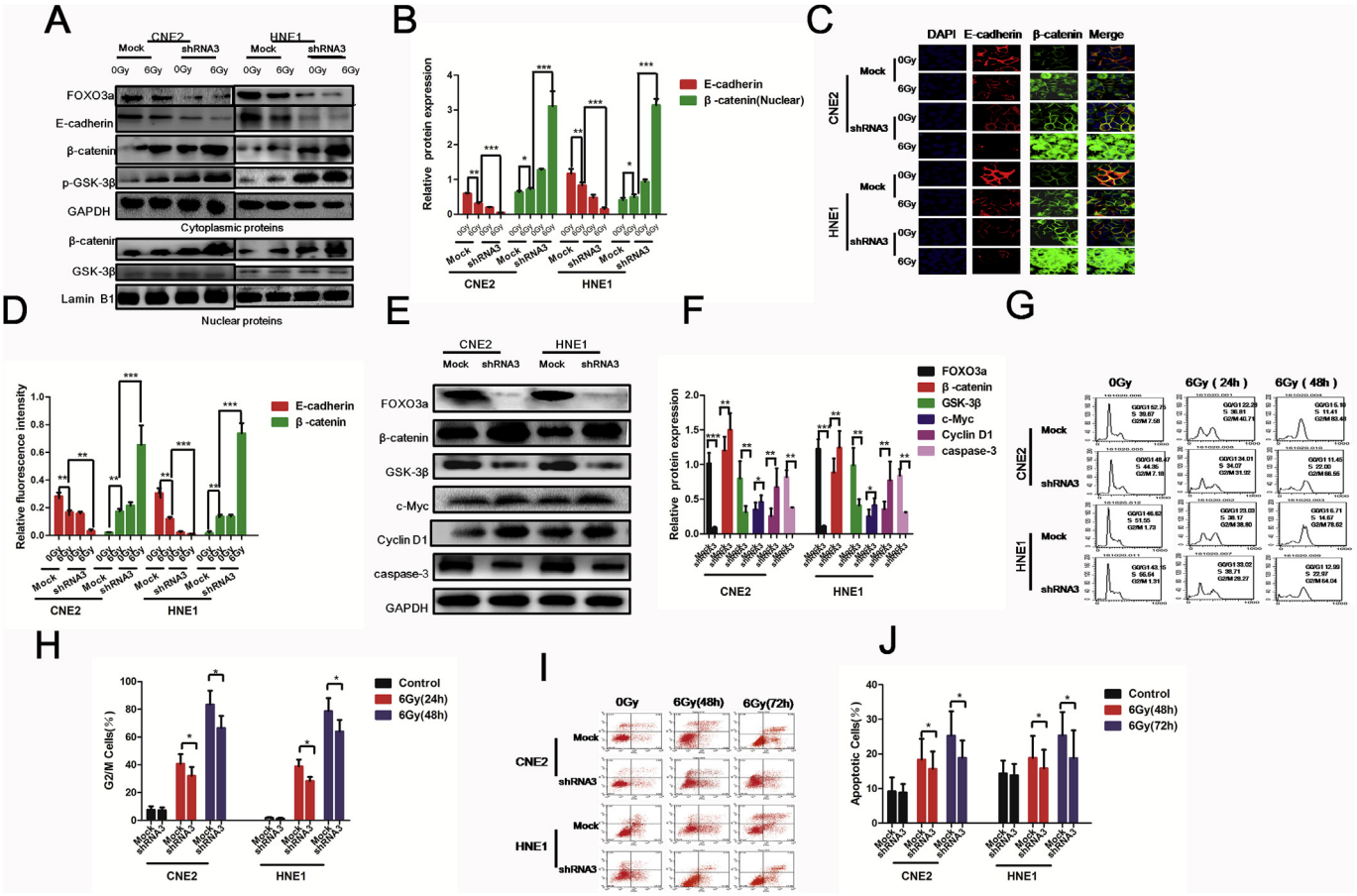

Fig. 3. Silencing of FOXO3a activates the Wnt/β-catenin signaling pathway in NPC cells. (A–B) Expression of FOXO3a, β-catenin, E-cadherin and p-GSK-3β in the cytoplasm, β-catenin and GSK-3β in the nucleus was determined using western blotting. (C–D) Immunofluorescence assays were used to determine the location of E-cadherin and β-catenin. (E–F) Expression of Wnt/β-catenin signaling pathway-related proteins was determined using western blotting. (G–H) Silencing of FOXO3a suppressed G2/M phase arrest in NPC cells. (I–J) Silencingof FOXO3a suppressed apoptosis in NPC cells. Error bars correspond to means ± standard deviations from three independent experiments.*P < 0.05 vs. control; **P < 0.01 vs. control; ***P < 0.005 vs. control.

Death Detection Kit, POD (11684817910, Roche, Switzerland) was used with terminal deoxynucleotidyl transferase-meditated dUTP-fluorescein nick end-labeling (TUNEL) to detect apoptosis. Brown granules in the cytoplasm, cell membrane, or nucleus were considered as positive staining.

2.14. Statistical analysis

Experiments were repeated independently at least three times. Data are shown as mean ± standard deviation (SD). Student's t-test and ANOVA were used for statistical analyses, and P < 0.05 was considered significant. *P < 0.05 vs. control; **P < 0.01 vs. control; ***P < 0.005 vs. control.

3. Results

3.1. Silencing FOXO3a induces radioresistance in NPC cells

To examine the expression of FOXO3a in NPC cells, western blotting and qRT-PCR were performed. The expression of FOXO3a was very similar in CNE1, CNE2, HNE1, and CNE1-LMP1 cells, but a lower expression of FOXO3a was found in CNE2R cells (Fig. 1A–C). Our preliminary results indicated that CNE2 and HNE1 are more suitable for radiotherapy-related experiments. Therefore, CNE2 and HNE1 cells were chosen for further study. We then investigated the role of FOXO3a in tumor radioresistance by knocking down its expression in NPC cells. We generated CNE2 and HNE1 cell lines in which FOXO3a was knocked down, and control CNE2 and HNE1 cells with mock shRNA, by transducing cells with mock shRNA, shRNA1, shRNA2, and shRNA3. Western blotting and qRT-PCR were then performed to confirm transduction efficiency. As shown in Fig. 1D–F, more than 70% FOXO3a was suppressed by each of the three shRNAs compared to mock shRNA. FOXO3a was more effectively reduced by shRNA3. Therefore, cells transduced with shRNA3 and mock shRNA were chosen for further experiments. The expression levels of FOXO family members were assessed using western blotting and qRT-PCR in irradiated NPC cells at different time points in Fig. 1G–I. The results show that FOXO3a expression decreased gradually after irradiation, while the expression of p-FOXO3a did not. However, other FOXO family members didn't respond to irradiation. The above data support the notion that FOXO3a could be induced by radiation in NPC. FOXO3a is phosphorylated by several upstream kinases, such as Akt, ERK, and SGK [25]. The phosphorylated form of the molecule is transferred from the nucleus by binding with 14–3-3 proteins and through exportins. In the cytoplasm, FOXO3a is further ubiquitinated and then degraded by an ubiquitin/proteasome-dependent manner [26]. Moreover, It has been well documented that radiation could activate these upstream kinases, which will in turn contribute to radioresistance in NPC [27–29]. Therefore, we speculate that radiation could lead to the loss of FOXO3a by activating these upstream kinases. The exact mechanism needs to be further explored. Engineered cell lines were then exposed to different doses of radiation for colony formation. ShRNA3 CNE2 and shRNA3 HNE1 cells had relatively higher colony survival rates compared to mock cells after irradiation (Fig. 1J-L) (P < 0.05). These results suggest that silencing

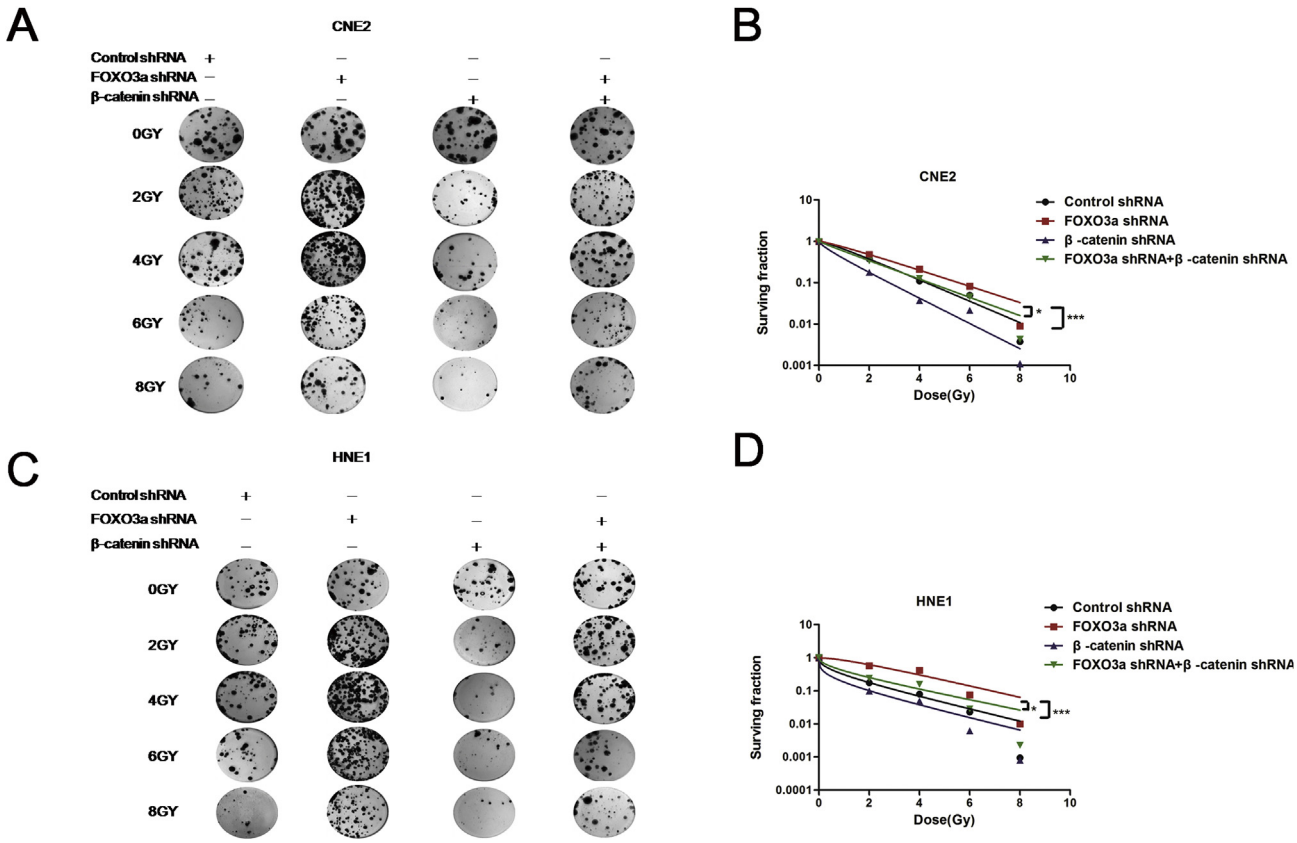

Fig. 4. Silencing of β-catenin reverses the radioresistance induced by FOXO3a shRNA in NPC cells. (A–D) Co-transducing β-catenin shRNA in NPC cell lines in which FOXO3a was silenced reversed the radioresistance induced by FOXO3a shRNA. Error bars correspond to means ± standard deviationsfrom three independent experiments. *P < 0.05 vs. control; **P < 0.01 vs. control; ***P < 0.005 vs. control.

FOXO3a induces radioresistance in NPC cells.

3.2. FOXO3a silencing induces EMT in NPC cells

To investigate the association between FOXO3a and EMT, western blotting was performed to detect alterations in EMT marker proteins after shRNA3 and mock shRNA transductions. Epithelial marker protein E-cadherin levels were reduced, whereas the levels of mesenchymal marker proteins vimentin and N-cadherin were increased in cells transduced with shRNA3 (Fig. 2A–B). We also used immunofluorescence to investigate the location of EMT marker proteins. We found that the amount of E-cadherin located in the cell membrane was reduced, whereas that of cytoplasmic vimentin was increased in cells transduced with shRNA3 (Fig. 2C–D). These results illustrate that silencing of FOXO3a may induce EMT in NPC cells. Scratch tests and transwell invasion experiments were also performed to verify the migration and invasion abilities of transduced cells. In scratch tests, the wound healing rate of shRNA3 CNE2 cells (68.71 ± 8.60%) was significantly increased compared to the mock group (40.71 ± 4.60%), with similar results for shRNA3 HNE1 cells (79.23 ± 8.60% vs. 52.71 ± 4.60%, P < 0.005) (Fig. 2E–F). We also found that silencing of FOXO3a enhanced the invasion ability of NPC cells as seen in the transwell experiments. The numbers of shRNA3 CNE2 and shRNA3 HNE1 cells passing through the extracellular matrix (ECM) gel and polycarbonate membrane were 289 ± 50 and 315 ± 61, respectively, compared with the mock CNE2 (168 ± 28) and mock HNE1 (135 ± 31) cells (Fig. 2G–H), and the difference was statistically significant (P < 0.005). We conclude that silencing of FOXO3a may induce EMT in NPC cells.

3.3. Silencing FOXO3a activates the Wnt/β-catenin signaling pathway in NPC cells

Under normal conditions, E-cadherin forms a complex with β-catenin at the cell membrane of epithelial cells [30]. During EMT, expression of E-cadherin in tumor cells is decreased or absent. When E-cadherin is reduced, β-catenin is released into the nucleus, activating its target genes and modulating the survival of tumor cells [31,32]. As shown in Fig. 3A–B, E-cadherin levels decreased after irradiation, whereas β-catenin levels in the nucleus increased, in shRNA3 FOXO3a cells compared with mock cells. On the other hand, GSK-3β inhibits tumor growth by degrading β-catenin. GSK-3β phosphorylation can inactivate GSK-3β and increase the nuclear localization of β-catenin, activating its target genes and modulating the survival of tumor cells [33,34]. We observed that an increase in the phosphorylation of GSK-3β could increase the levels of β-catenin. However, there was no significant change in the nuclear localization of GSK-3β. These results were confirmed by immunofluorescence as shown in Fig. 3C–D. We conclude that irradiation induces EMT and reduces the expression of E-cadherin, which would cause an increase in nuclear levels of β-catenin. After FOXO3a knockdown, β-catenin levels in the nucleus increased more significantly than in mock cells. In addition, Wnt/β-catenin signaling pathway-related genes were found to be activated after silencing of FOXO3a (Fig. 3E–F). Numerous studies have shown that β-catenin influences cell cycle distribution and apoptosis by modulating its target genes [35,36], and cell cycle distribution and apoptosis plays a vital role in radioresistance in different cancers [37]. Our previous experiments have shown that FOXO3a regulates the expression of β-catenin and its target genes. Therefore, flow cytometry was used to determine whether silencing FOXO3a could suppress G2/M arrest and apoptosis, which in turn would increase radioresistance in NPC cells. As shown in

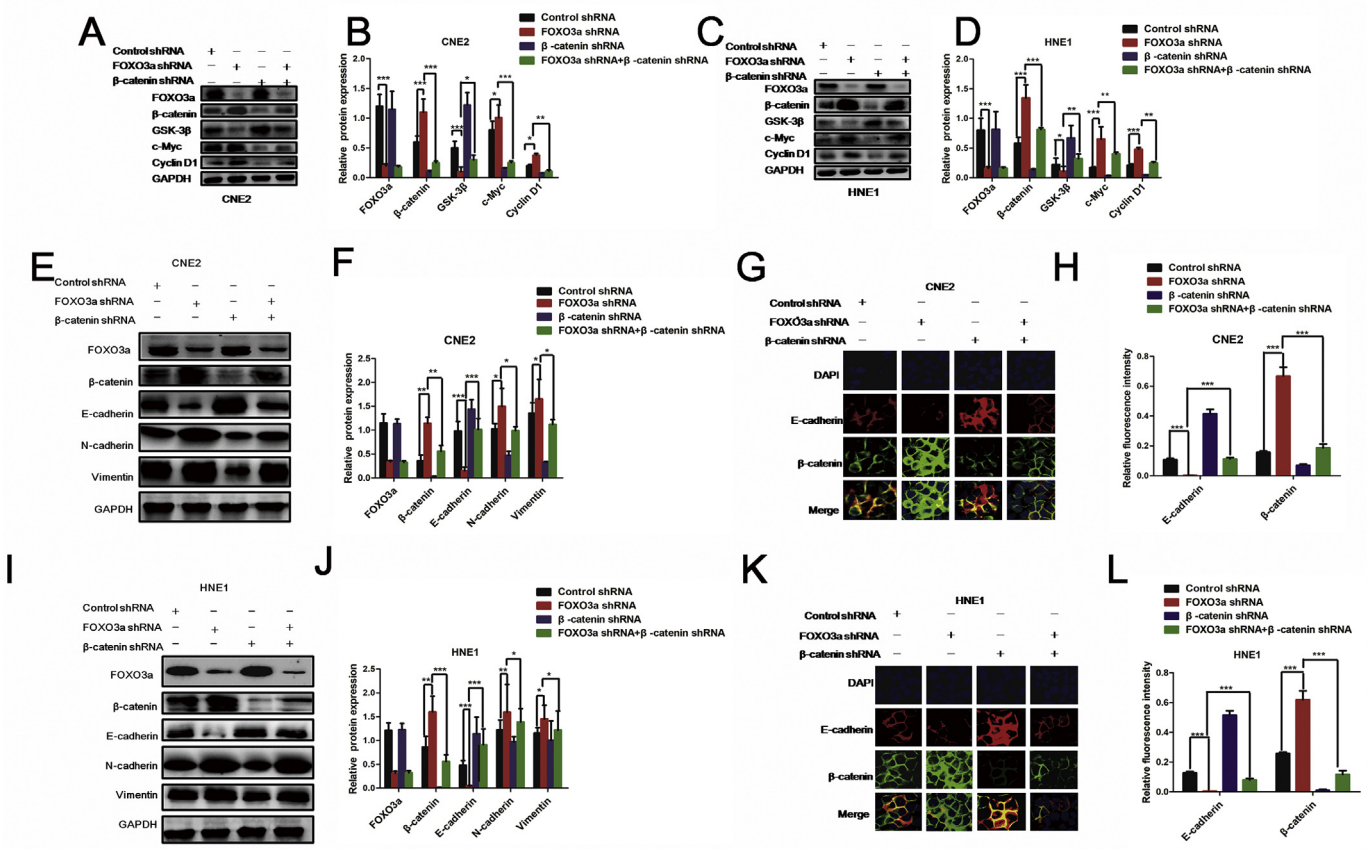

Fig. 5. Silencingof β-catenin reverses activation of the Wnt/β-catenin signaling pathway and EMT induced by FOXO3a shRNA in NPC cells. (A–D) Co-transducing β-catenin shRNA in NPC cell lines in which FOXO3a was silenced reversed the changes in downstream genes induced by FOXO3a shRNA. (E–L) Co-transducing β-catenin shRNA in NPC cell lines in which FOXO3a was silenced reversed the EMT induced by FOXO3a shRNA. Error bars correspond to means ± standard deviations from three independent experiments. *P < 0.05 vs. control; **P < 0.01 vs. control; ***P < 0.005 vs. control.

Fig. 3G–H, irradiation resulted in a G2/M phase arrest in NPC cells, and the proportion of G2/M phase cells increased with longer irradiation. FOXO3a gene knockdown significantly reduced the proportion of cells arrested in G2/M compared to mock cells (Fig. 3G–H) (HNE1, $P < 0.05$; CNE2, $P < 0.05$). We confirmed that G2/M phase cells are sensitive to radiation, whereas S phase cells appear to be resistant. Thus, silencing of FOXO3a could decrease the number of NPC cells in the sensitive G2/M stage, which might result in radioresistance. As shown in Fig. 3I–J, irradiation increased the frequency of apoptosis in NPC cells. After FOXO3a knockdown, the proportion of apoptotic cells significantly decreased compared to mock cells (HNE1, $P < 0.05$; CNE2, $P < 0.05$). These results suggest that silencing FOXO3a activates the Wnt/β-catenin signaling pathway and suppresses G2/M arrest and apoptosis in NPC cells.

3.4. β-Catenin silencing reverses radioresistance induced by FOXO3a shRNA in NPC cells

We next investigated whether β-catenin shRNA could reverse the radioresistance induced by FOXO3a shRNA in NPC cells. β-Catenin shRNA was transduced in NPC cell lines in which FOXO3a was silenced. Colony formation assay results showed that co-transducing β-catenin shRNA could reverse the radioresistance induced by FOXO3a shRNA (Fig. 4A–D). These results suggest that silencing FOXO3a induces radioresistance by activating the Wnt/β-catenin signaling pathway in NPC cells.

3.5. β-Catenin silencing reverses activation of the Wnt/β-catenin signaling pathway and EMT induced by FOXO3a shRNA in NPC cells

To explore the underlying mechanism of how FOXO3a shRNA regulates radioresistance by modulating β-catenin, the expression levels of Wnt/β-catenin signaling pathway-and EMT-associated proteins were determined. The results show that silencing of FOXO3a increased the expression of β-catenin, whereas silencing of β-catenin had no effect on FOXO3a expression levels (Fig. 5A–D). Previous studies have shown that activation of the Wnt/β-catenin signaling pathway induces EMT [38,39], and our results have shown that silencing of FOXO3a activates the Wnt/β-catenin signaling pathway in NPC cells. To determine whether silencing β-catenin could reverse the EMT induced by FOXO3a shRNA in NPC cells, western blotting and immunofluorescence assays were performed to detect alterations in EMT marker proteins. We found that silencing β-catenin reverses the EMT induced by FOXO3a shRNA in NPC cells (Fig. 5E-L). These results indicate that FOXO3a, the Wnt/β-catenin signaling pathway, and EMT could form a positive feedback regulatory network in NPC cells.

3.6. FOXO3a silencing promotes radioresistance in a xenograft model

A xenograft mouse model was employed to further validate whether silencing FOXO3a could promote radioresistance *in vivo*. The tumor sizes were larger and growth rates were higher in CNE2-shRNA3 compared to CNE2-Mock groups (Fig. 6A–C). After receiving 8 Gy of irradiation, irradiated groups had a significantly lower rate of tumor growth than non-irradiated groups. In addition, the tumor size in CNE2 shRNA3 groups after 8 Gy of irradiation was larger than in irradiated

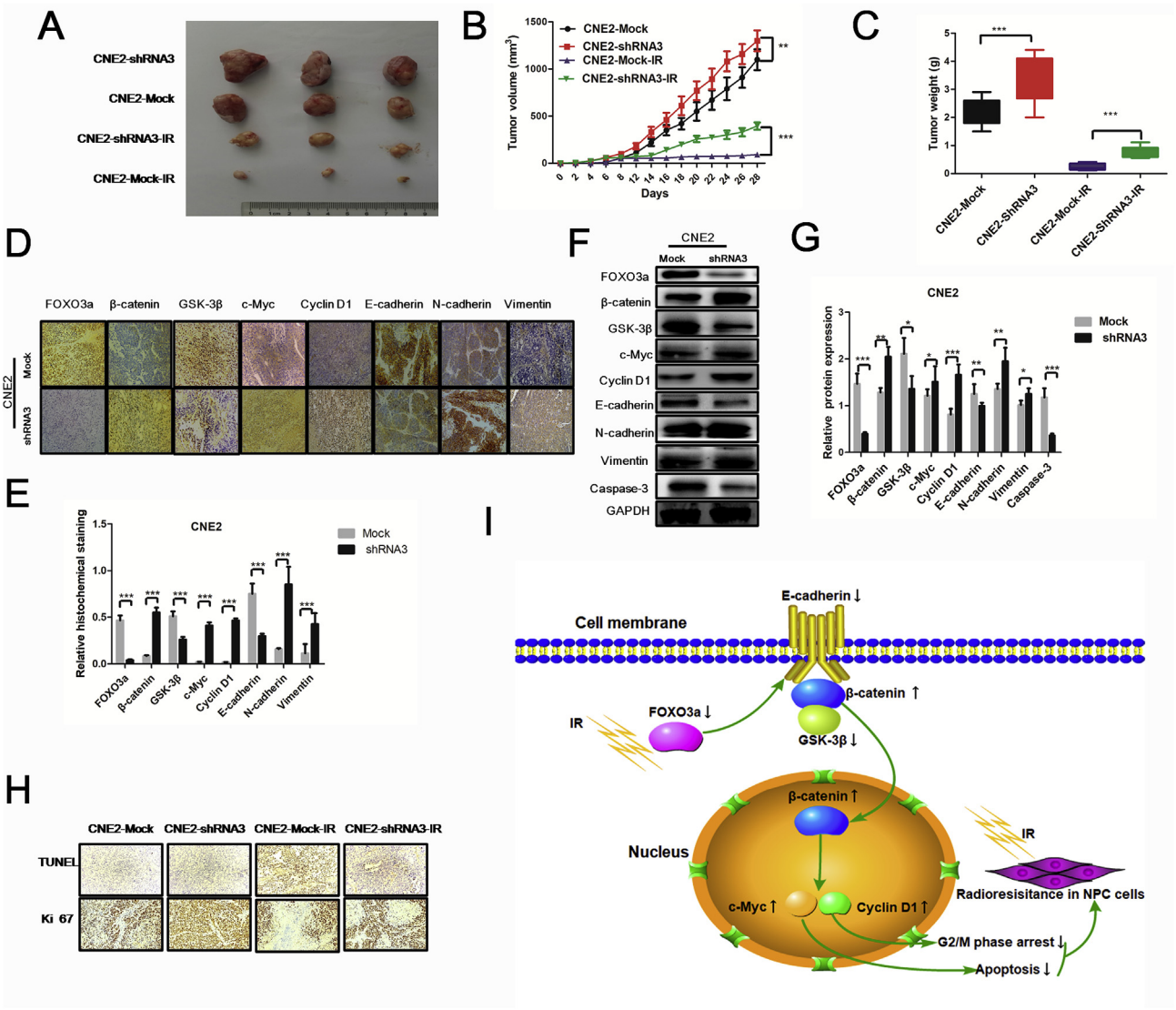

Fig. 6. Silencing of FOXO3a promotes tumor radioresistance in a xenograft model. (A)Tumor volumes from each group were tracked for 28 days; the representative tumor samples from each group are shown. (B) Tumor growth rate in each group. (C) Tumor weight in each group. (D–E) Representative immunohistochemical staining of FOXO3a, EMT-related proteins, Wnt/β-catenin signaling pathway-related proteins and caspase-3 from tumor samples in each non-irradiated group (magnification: 200 ×). (F–G) Expression of F FOXO3a, EMT-related proteins, Wnt/β-catenin signaling pathway-related proteins and caspase-3 were determined using western blotting. (H) Representative immunohistochemical staining of TUNEL and Ki-67 from tumor samples in each group (magnification: 200 ×). (I) Flowchart of our experiments. Error bars correspond to means ± standard deviations from three independent experiments. *P < 0.05 vs. control; **P < 0.01 vs. control; ***P < 0.005 vs. control.

mock groups (Fig. 6A–C). Furthermore, three specimens were randomly selected from each group for Western blot and immunohistochemical detection. Silencing of FOXO3a could induce EMT *in vivo*, as evident by the downregulation of E-cadherin and the upregulation of vimentin and N-cadherin. Moreover, we found that silencing FOXO3a could activate the Wnt/β-catenin signaling pathway *in vivo* through detecting the pathway-related genes. Furthermore, silencing FOXO3a could suppress the expression of the apoptotic marker caspase-3 (Fig. 6D–G). Increased Ki-67 signals were observed in the shRNA3 groups compared to the mock groups suggesting that FOXO3a knockdown could promote tumor invasiveness *in vivo*. In addition, TUNEL assay found that knockdown of FOXO3a could suppress apoptosis *in vivo*. (Fig. 6H). These data together indicate that silencing FOXO3a induces radioresistance by promoting EMT and activating the Wnt/β-catenin signaling pathway *in vivo*. A flowchart of our experiments is shown in Fig. 6I.

4. Discussion

With the rapid development of radiotherapy technology and chemotherapy regimens, the 5-year survival rate of NPC has reached approximately 80% [1]. Radiotherapy is the major therapeutic modality used to treat NPC. Although NPC is sensitive to radiotherapy, a major impediment to achieve long-term survival is radioresistance, which has been linked to an increased likelihood of recurrence and distant metastasis [2]. Our study confirmed that silencing of FOXO3a triggers an EMT-like phenotypic transition in NPC cells. Induction of EMT leads to a downregulation in the expression of E-cadherin, increased levels of β-catenin in the nucleus, and activation of the Wnt/β-catenin signaling pathway [31,32]. β-Catenin is a key component of the Wnt signaling pathway and can translocate to the nucleus, serving as a transcriptional factor that causes radioresistance in NPC [40]. Our studies confirmed that radiation promotes accumulation of β-catenin in the nucleus, and that FOXO3a knockdown clearly enhances this accumulation. The downstream target genes of β-catenin have been identified as playing

an important role in the cell cycle and apoptosis [37]. Our results show that silencing FOXO3a suppresses apoptosis and reduces G2/M arrest in NPC cells. Moreover, silencing β-catenin could reverse activation of the Wnt/β-catenin signaling pathway and EMT induced by FOXO3a knockdown in NPC cells. Our results suggest that silencing FOXO3a leads to acquired radioresistance in NPC by inducing EMT and activating the Wnt signaling pathway.

Shou et al. reported that tumors with low FOXO3a expression were more frequently detected in advanced clinical stages, high T stages, lymph node metastasis, and distant metastasis in NPC [7]. However, the underlying mechanism was not explored. The present work represents the first systematic investigation on the effects of FOXO3a knockdown on the emerging radioresistance in an in vitro NPC model and a xenograft model. The results provide a new approach to overcome radioresistance in NPC.

To date, studies on the role of FOXO3a in tumorigenesis are controversial. Some groups reported that activation of FOXO3a reverses the invasive phenotype in cancer cells, and downregulation of FOXO3a promotes tumorigenesis [16,41]. In contrast, other groups reported that FOXO3a could serve as an oncogene [42,43]. These findings suggest the multifaceted mechanisms of FOXO3a signaling under different cellular contexts. Our study shows that FOXO3a is a tumor suppressor gene in NPC, which increases our understanding of its role in tumorigenesis. Our results are consistent with a previous study in NPC [7].

Latent membrane protein-1 (LMP1) is the principal EBV oncoprotein. NPC with a high level of LMP1 expression are reported to exhibit an increased tendency toward metastasis compared with those with lower levels of LMP1 expression [44,45]. It has been demonstrated that the EMT is induced by LMP1 and is associated with metastatic in NPC [46,47]. CNE1-LMP1 used in our experiment is established by introducing LMP1 cDNA into CNE1 cells. In Fig. 1A, the expression of FOXO3a was identified and no difference was found between CNE1-LMP1 and other NPC cell lines. Moreover, we found that CNE1 and CNE1-LMP1 cell had poorer ability to form clones than CNE2 and HNE1 after radiation in Supplementary Fig. 1. This result is different from that the results of Ya Cao and his team, which may be due to cell senescence caused by repeated cell digestion and passage [48]. So CNE2 and HNE1 were chosen for further research. In another study, CNE2-LMP1 was also used as a cell model to study the contribution of viral protein in readioresistance of NPC cells [49]. Owning to lack of CNE2-LMP1 cell line in our medical center, we established CNE2-LMP1 cell line by introducing LMP1 cDNA into CNE2 cells and identifying its transfection efficiency in Supplementary Fig. 2. Moreover, the expression of FOXO3a was detected between CNE2, CNE2-control and CNE2-LMP1 by western blotting and qRT-PCR. The expression of FOXO3a was very similar in CNE2, CNE2-control and CNE2-LMP1 in Supplementary Fig. 3. The Cancer Genome Atlas HNSCC database was applied to identify the correlation between FOXO3a and LMP1, and no significant correlation was detected in Supplementary Fig. 4. In conclusion, we speculate that FOXO3a might regulate NPC cells not related to EBV oncoprotein LMP1. The inner mechanism needs to be further explored. However, in the present study, we mainly focused on the promotion of radioresistance in NPC regulated by the FOXO3a, and we think that our experiment at present may not be optimal, but should be sufficient to draw a conclusion that FOXO3a knockdown could promote radioresistance in nasopharyngeal carcinoma by inducing EMT and the Wnt/β-catenin signaling pathway. However, in the present study, we mainly focused on the promotion of radioresistance in NPC regulated by the FOXO3a, and we think that our experiment at present may not be optimal, but should be sufficient to draw a conclusion that FOXO3a knockdown could promote radioresistance in nasopharyngeal carcinoma by inducing EMT and the Wnt/β-catenin signaling pathway. Moreover, limitations of our study include lack of tissues from patients and lack of long-term follow-up data. Nevertheless, our results provide a useful hypothesis for future trials.

We plan to further clarify the underlying mechanisms and provide more evidence for radioresistance in NPC in a future work. In combination with previous reports, we expect that our findings on the functional interaction of FOXO3a with β-catenin will provide useful information for the development of effective therapies against NPC.

Author contributions

GYH and GQH conceived the idea. ML, CW, EGG, SP, XN, LLZ, WS, and DBL performed the experiments. ML, CW, and EGG analyzed the data. ML and CW wrote the manuscript. All authors approved the final version of the manuscript.

Conflicts of interest

The authors declare no conflict of interest.

Acknowledgments

This work was supported by the National Natural Science Foundation of China (81572960, 81773231).

Appendix A. Supplementary data

Supplementary data to this article can be found online at https://doi.org/10.1016/j.canlet.2019.04.019.

References

[1] M.L. Chua, J.T. Wee, E.P. Hui, A.T. Chan, Nasopharyngeal carcinoma, Lancet 387 (2016) 1012–1024.
[2] A.W. Lee, B.B. Ma, W.T. Ng, A.T. Chan, Management of nasopharyngeal carcinoma: current practice and future perspective, J. Clin. Oncol. 33 (2015) 3356–3364.
[3] I.W. Tham, J.J. Lu, Controversies and challenges in the current management of nasopharyngeal cancer, Expert Rev. Anticancer Ther. 10 (2010) 1439–1450.
[4] Y. Wang, Y. Zhou, FOXO transcription factors: their clinical significance and regulation, BioMed Res. Int. 2014 (2014) 925350.
[5] V.D.V. Ke, P.J. Coffer, The extending network of FOXO transcriptional target genes, Antioxidants Redox Signal. 14 (2011) 579.
[6] R.S. Nho, P. Hergert, FoxO3a and disease progression, World J. Biol. Chem. 5 (2014) 346–354.
[7] Z. Shou, L. Lin, J. Liang, J.L. Li, H.Y. Chen, Expression and prognosis of FOXO3a and HIF-1alpha in nasopharyngeal carcinoma, J. Cancer Res. Clin. Oncol. 138 (2012) 585–593.
[8] J. Zhang, X. Wen, X.Y. Ren, Y.Q. Li, X.R. Tang, Y.Q. Wang, Q.M. He, X.J. Yang, Y. Sun, N. Liu, J. Ma, YPEL3 suppresses epithelial-mesenchymal transition and metastasis of nasopharyngeal carcinoma cells through the Wnt/beta-catenin signaling pathway, J. Exp. Clin. Cancer Res. 35 (2016) 109.
[9] S.L. Liu, H.X. Lin, C.Y. Lin, X.Q. Sun, L.P. Ye, F. Qiu, W. Wen, X. Hua, X.Q. Wu, J. Li, L.B. Song, L. Guo, TIMELESS confers cisplatin resistance in nasopharyngeal carcinoma by activating the Wnt/beta-catenin signaling pathway and promoting the epithelial mesenchymal transition, Cancer Lett. 402 (2017) 117–130.
[10] P.G. Santamaria, G. Moreno-Bueno, F. Portillo, A. Cano, EMT: present and future in clinical oncology, Mol Oncol 11 (2017) 718–738.
[11] H. Liu, J. Yin, H. Wang, G. Jiang, M. Deng, G. Zhang, X. Bu, S. Cai, J. Du, Z. He, FOXO3a modulates WNT/beta-catenin signaling and suppresses epithelial-to-mesenchymal transition in prostate cancer cells, Cell. Signal. 27 (2015) 510–518.
[12] Y. Liu, X. Ao, W. Ding, M. Ponnusamy, W. Wu, X. Hao, W. Yu, Y. Wang, P. Li, J. Wang, Critical role of FOXO3a in carcinogenesis, Mol cancer 17 (2018) 104.
[13] H. Hu, G. Wang, C. Li, miR-124 suppresses proliferation and invasion of nasopharyngeal carcinoma cells through the Wnt/beta-catenin signaling pathway by targeting Capn4, OncoTargets Ther. 10 (2017) 2711–2720.
[14] J. Wang, M. Kang, Q. Wen, Y.T. Qin, Z.X. Wei, J.J. Xiao, R.S. Wang, Berberine sensitizes nasopharyngeal carcinoma cells to radiation through inhibition of Sp1 and EMT, Oncol. Rep. 37 (2017) 2425–2432.
[15] S.U. Zhongwu, L.I. Guo, L. Chao, S. Ren, Y. Tian, L. Yong, Y. Qiu, Ionizing radiation promotes advanced malignant traits in nasopharyngeal carcinoma via activation of epithelial-mesenchymal transition and the cancer stem cell phenotype, Oncol. Rep. 36 (2016) 72–78.
[16] D. Ni, X. Ma, H.Z. Li, Y. Gao, X.T. Li, Y. Zhang, Q. Ai, P. Zhang, E.L. Song, Q.B. Huang, Y. Fan, X. Zhang, Downregulation of FOXO3a promotes tumor metastasis and is associated with metastasis-free survival of patients with clear cell renal cell carcinoma, Clin. Cancer Res. 20 (2014) 1779–1790.
[17] M. Lam, A.R. Carmichael, H.R. Griffiths, An aqueous extract of Fagonia cretica induces DNA damage, cell cycle arrest and apoptosis in breast cancer cells via FOXO3a and p53 expression, PLoS One 7 (2012) e40152.
[18] T. Kajihara, M. Jones, L. Fusi, M. Takano, F. Feroze-Zaidi, G. Pirianov, H. Mehmet, O. Ishihara, J.M. Higham, E.W. Lam, Differential expression of FOXO1 and FOXO3a

confers resistance to oxidative cell death upon endometrial decidualization, Mol. Endocrinol. 20 (2006) 2444–2455.
[19] R. Wang, Q. Yang, X. Wang, W. Wang, J. Li, J. Zhu, X. Liu, J. Liu, J. Du, FoxO3alpha-mediated autophagy contributes to apoptosis in cardiac microvascular endothelial cells under hypoxia, Microvasc. Res. 104 (2016) 23–31.
[20] X. Pan, J. Mou, S. Liu, Z. Sun, R. Meng, Z. Zhou, G. Wu, G. Peng, SHP-1 overexpression increases the radioresistance of NPC cells by enhancing DSB repair, increasing S phase arrest and decreasing cell apoptosis, Oncol. Rep. 33 (2015) 2999–3005.
[21] S.L. Lomonaco, S. Finniss, C. Xiang, A. Decarvalho, F. Umansky, S.N. Kalkanis, T. Mikkelsen, C. Brodie, The induction of autophagy by γ-radiation contributes to the radioresistance of glioma stem cells, Int. J. Cancer 125 (2009) 717.
[22] Y. Tamari, G. Kashino, H. Mori, Acquisition of radioresistance by IL-6 treatment is caused by suppression of oxidative stress derived from mitochondria after γ-irradiation, J. Radiat. Res. (2017) 1.
[23] R. Glaser, H.Y. Zhang, K.T. Yao, H.C. Zhu, F.X. Wang, G.Y. Li, D.S. Wen, Y.P. Li, Two epithelial tumor cell lines (HNE-1 and HONE-1) latently infected with Epstein-Barr virus that were derived from nasopharyngeal carcinomas, Proc. Natl. Acad. Sci. U. S. A. 86 (1989) 9524–9528.
[24] Z. Yan, T. Yong-Guang, L. Fei-Jun, T. Fa-Qing, T. Min, C. Ya, Interference effect of epigallocatechin-3-gallate on targets of nuclear factor kappaB signal transduction pathways activated by EB virus encoded latent membrane protein 1, Int. J. Biochem. Cell Biol. 36 (2004) 1473–1481.
[25] J.P. Guo, W. Tian, S. Shu, Y. Xin, C. Shou, J.Q. Cheng, IKBKE phosphorylation and inhibition of FOXO3a: a mechanism of IKBKE oncogenic function, PLoS One 8 (2013) e63636.
[26] Y.Q. Wang, Q. Cao, F. Wang, L.Y. Huang, T.T. Sang, F. Liu, S.Y. Chen, SIRT1 protects against oxidative stress-induced endothelial progenitor cells apoptosis by inhibiting FOXO3a via FOXO3a ubiquitination and degradation, J. Cell. Physiol. 230 (2015) 2098–2107.
[27] C.S. Kim, J.K. Kim, S.Y. Nam, K.H. Yang, M. Jeong, H.S. Kim, C.S. Kim, Y.W. Jin, J. Kim, Low-dose radiation stimulates the proliferation of normal human lung fibroblasts via a transient activation of Raf and Akt, Mol. Cell. 24 (2007) 424–430.
[28] A.T.Y. Chen, C. Guo, K.J. Dumas, K. Ashrafi, P.J. Hu, Effects of Caenorhabditis elegans sgk-1 mutations on lifespan, stress resistance, and DAF-16/FoxO regulation, 5 (2013-07-19), 12, Aging Cell 12 (2013) 932–940.
[29] F.R. Tang, W.K. Loke, Molecular mechanisms of low dose ionizing radiation-induced hormesis, adaptive responses, radioresistance, bystander effects, and genomic instability, Int. J. Radiat. Biol. 91 (2015) 1–15.
[30] X. Tian, Z. Liu, B. Niu, J. Zhang, T.K. Tan, S.R. Lee, Y. Zhao, D.C. Harris, G. Zheng, E-cadherin/beta-catenin complex and the epithelial barrier, J. Biomed. Biotechnol. 2011 (2011) 567305.
[31] R. Karim, G. Tse, T. Putti, R. Scolyer, S. Lee, The significance of the Wnt pathway in the pathology of human cancers, Pathology 36 (2004) 120–128.
[32] M.J. Smalley, T.C. Dale, Wnt signalling in mammalian development and cancer, Cancer Metastasis Rev. 18 (1999) 215–230.
[33] Y. Fu, S. Zheng, N. An, T. Athanasopoulos, L. Popplewell, A. Liang, K. Li, C. Hu, Y. Zhu, beta-catenin as a potential key target for tumor suppression, Int. J. Cancer 129 (2011) 1541–1551.
[34] S. Nagini, J. Sophia, R. Mishra, Glycogen synthase kinases: moonlighting proteins with theranostic potential in cancer, Semin. Canc. Biol. (2018), https://doi.org/10.1016/j.semcancer.2017.12.010.
[35] B.S. Xie, X.X. He, Z.L. Ai, S.K. Yao, Involvement of beta-catenin in matrine-induced autophagy and apoptosis in WB-F344 cells, Mol. Med. Rep. 9 (2014) 2547–2553.
[36] J. Zhang, A.J. Gill, J.D. Issacs, B. Atmore, A. Johns, L.W. Delbridge, R. Lai, T.P. Mcmullen, The Wnt/β-catenin pathway drives increased cyclin D1 levels in lymph node metastasis in papillary thyroid cancer, Hum. Pathol. 43 (2012) 1044–1050.
[37] Y.F. Yuan, D.J. Wang, Y.B. Pan, G. Liang, J. Xiao, S.M. Wang, H.L. Yang, Curcumin analogue B67 induces apoptosis and G_2/M arrest to suppress radioresistant nasopharyngeal carcinoma cells, Chin. J. Pathol. 27 (2011) 504–508.
[38] Y. Gu, Q. Wang, K. Guo, W. Qin, W. Liao, S. Wang, Y. Ding, J. Lin, TUSC3 promotes colorectal cancer progression and epithelial-mesenchymal transition (EMT) through WNT/β-catenin and MAPK signalling, J. Pathol. 239 (2016) 60.
[39] R. Nusse, H. Clevers, Wnt/beta-Catenin signaling, disease, and emerging therapeutic modalities, Cell 169 (2017) 985–999.
[40] G. Li, Y. Wang, Y. Liu, Z. Su, C. Liu, S. Ren, T. Deng, D. Huang, Y. Tian, Y. Qiu, miR-185-3p regulates nasopharyngeal carcinoma radioresistance by targeting WNT2B in vitro, Cancer Sci. 105 (2014) 1560–1568.
[41] S.K. Ananda Sadagopan, N. Mohebali, C.Y. Looi, M. Hasanpourghadi, A.K. Pandurangan, A. Arya, H. Karimian, M.R. Mustafa, Forkhead Box Transcription Factor (FOXO3a) mediates the cytotoxic effect of vernodalin in vitro and inhibits the breast tumor growth in vivo, J. Exp. Clin. Cancer Res. 34 (2015) 147.
[42] K. Xu, H. Pei, Z. Zhang, S. Dong, R.J. Fu, W.M. Wang, H. Wang, FoxO3a mediates glioma cell invasion by regulating MMP9 expression, Oncol. Rep. 36 (2016) 3044–3050.
[43] S. Yu, Y. Yu, W. Zhang, W. Yuan, N. Zhao, Q. Li, Y. Cui, Y. Wang, W. Li, Y. Sun, T. Liu, FOXO3a promotes gastric cancer cell migration and invasion through the induction of cathepsin L, Oncotarget 7 (2016) 34773–34784.
[44] K. Shair, A. Reddy, V.S. Cooper, New insights from elucidating the role of LMP1 in nasopharyngeal carcinoma, Cancers 10 (2018) 86.
[45] Y. Tomokazu, K. Satoru, W. Naohiro, M. Shigeyuki, E. Kazuhira, S. Hisashi, N. Sayaka, T. Akira, I. Makoto, Pathogenic role of Epstein-Barr virus latent membrane protein-1 in the development of nasopharyngeal carcinoma, Cancer Lett. 337 (2013) 1–7.
[46] M.T. Liu, Y.S. Chen, C.Y. Hu, C.S. Lin, Y.T. Chang, W.B. Wang, J.Y. Chen, Epstein-Barr virus latent membrane protein 1 induces micronucleus formation, represses DNA repair and enhances sensitivity to DNA-damaging agents in human epithelial cells, Oncogene 23 (2004) 2531–2539.
[47] H. Toshiyuki, Y. Jing, K. Satoru, Y. Tomokazu, J. Irene, F. Mitsuru, J.S. Pagano, Twist and epithelial-mesenchymal transition are induced by the EBV oncoprotein latent membrane protein 1 and are associated with metastatic nasopharyngeal carcinoma, Cancer Res. 67 (2007) 1970.
[48] J. Lu, M. Tang, H. Li, Z. Xu, X. Weng, J. Li, X. Yu, L. Zhao, H. Liu, Y. Hu, Z. Tan, L. Yang, M. Zhong, J. Zhou, J. Fan, A.M. Bode, W. Yi, J. Gao, L. Sun, Y. Cao, EBV-LMP1 suppresses the DNA damage response through DNA-PK/AMPK signaling to promote radioresistance in nasopharyngeal carcinoma, Cancer Lett. 380 (2016) 191–200.
[49] C.F. Yang, L.X. Peng, T.J. Huang, G.D. Yang, Q.Q. Chu, Y.Y. Liang, X. Cao, P. Xie, L.S. Zheng, H.B. Huang, M.D. Cai, J.L. Huang, R.Y. Liu, Z.Y. Zhu, C.N. Qian, B.J. Huang, Cancer stem-like cell characteristics induced by EB virus-encoded LMP1 contribute to radioresistance in nasopharyngeal carcinoma by suppressing the p53-mediated apoptosis pathway, Cancer Lett. 344 (2014) 260–271.